

5 Modeling Active Dendritic Processes in Pyramidal Neurons

Zachary F. Mainen and Terrence J. Sejnowski

5.1 Introduction

The role of active ion channels in dendritic function is among the most interesting and complex aspects of information processing in single neurons (reviewed in Mel 1994; Segev, Rinzel, and Shepherd 1995; Yuste and Tank 1996; Johnston et al. 1996; Koch 1997, Borg-Graham, 1997). While the behavior of isolated channels or the passive electrical properties of dendrites can be studied in isolation, the interaction of multiple nonlinear ionic currents within a geometrically complex structure is described by equations that cannot be solved analytically and often resist intuition. Detailed computer models thus provide a crucially needed framework within which hypotheses about active dendritic mechanisms can be expressed and tested. Realistic neuronal models help determine whether known biophysical properties can account for experimental observations and provide insight into computational functions of these mechanisms.

The chief obstacle in constructing such models is obtaining constraints for their parameters. Until recently, not enough experimental data were available on the physiological properties of cortical neurons to be able to create accurate models. In early models of hippocampal and neocortical neurons (e.g., Traub and Llinás 1979; Shepherd et al. 1985; Bernander et al. 1991; Lytton and Sejnowski 1991), the kinetic properties of the channels were mixed and matched from cortical and noncortical neurons, including motoneurons in the spinal cord, sympathetic ganglion cells, and even the squid giant axon. Still scantier data were available regarding the spatial distribution of channels present in dendrites, axons, and synaptic terminals. Fortunately, the application of dendritic patch recordings, Ca^{2+} imaging, and immunocytochemistry and other molecular techniques is now yielding an abundance of precise data on the properties and localization of ion channels in the dendritic membrane. Furthermore, dendritic recordings and imaging of Ca^{2+} - or voltage-sensitive dyes provide windows into dendritic behavior not available with traditional somatic recordings. Thus the time is ripe for detailed models of active dendritic computation.

The basics of compartmental models are presented in chapter 3, this volume, and numerical methods for solving them in chapter 14. In the present chapter, we show how compartmental simulations can be used to model neurons with active dendritic ion channels; our focus is chiefly on modeling pyramidal neurons such as those of the neocortex and hippocampus, but much of the material can be applied more widely. In section 5.2, we present definitions of channel types, their densities, and their localization, and we discuss the steps involved in combining experimental data into a

model of an active, spatially extended neuron. In section 5.3, we present applications, concentrating on models that exemplify the close interactions possible between simulations and physiology. Finally, in section 5.4, we discuss techniques for simplifying and analyzing complex models.

5.2 Passive Cable Models

Compartmental modeling (Rall 1964; Segev, Rinzel, and Shepherd 1994 and chapter 2, this volume) provides a general framework within which chemical and electrical signaling can be described at the level of single neurons. The strategy of this technique is to approximate the partial differential cable equations using both spatial and temporal discretization (see chapter 2, this volume). The advantage of this strategy over analytical techniques is that arbitrary geometries and ionic currents can be included and examined. The disadvantages are that simulations of complex dendritic geometries can be highly computation-intensive and that the parameters to be measured or estimated are legion (see section 5.2.6 on exploring parameters). Two high-quality public domain compartmental simulation environments are available: NEURON (Hines and Carnevale 1997; and chapter 3, this volume) and GENESIS (Bower and Beeman 1995; and chapter 12, this volume). Both provide efficient techniques for numerical solution of the cable equations as well as powerful languages and convenient graphic interfaces for programming and controlling the simulations. (For an introduction to NEURON, used for some of the simulations presented in this chapter, see the appendix to chapter 3, this volume.)

The first task in developing a model is to determine the structure of the neuron and the behavior of its ion channels (see chapter 3, this volume, for a general discussion of the passive properties of neurons and the influence of the various parameters on the cable properties of branched structures). Section 5.2 will focus on how the neuronal morphology is specified and on recent estimates for the properties and densities of voltage-dependent ion channels in cortical neurons, a subject that is rapidly changing as more data become available.

5.2.1 Passive Electrical Structure

Geometry Whereas in a single-compartment model, all channel currents combine linearly to produce a total membrane current, in a spatially extended neuron, the electrotonic structure of the neuron defines a much more complex spatiotemporal interplay between ion channels. The specification of the linear cable properties can be considered the first step in defining an active model and here entails translating

a neuroanatomical description into a set of discrete connected compartments. In NEURON, these are cylinders with specified lengths, "L," and diameters, "diam."

Because the choice of compartment size ("segment" size in NEURON) will affect the accuracy of a compartmental simulation (Hines and Carnevale 1997), care must be taken to choose a sufficiently fine discretization to avoid numerical errors. In simulations with active currents that can be much faster or more localized than the passive currents, there is no absolute rule for an adequate spatial discretization. A compartment size no larger than 0.05λ has been suggested (Cooley and Dodge 1966; De Schutter and Bower 1994a). As in temporal discretization, "dt," a good strategy is to compare the results at a given maximum compartment length with the those at a finer discretization (e.g., doubling the number of compartments). As the number of compartments increases, the quantitative results from the simulations should converge, indicating that the compartment size is sufficiently small.

Although most models begin with a reconstructed neuron in the form of a computer file, it is worth enumerating the factors one should consider in evaluating such digitized anatomical data. Although care in reconstruction is obviously most important, albeit somewhat difficult to evaluate from the finished product, there are a number of other important factors that go into accurately representing a dendritic arbor from a dye-filled neuron. These factors can have a considerable effect on the ultimate electrical structure of the modeled neuron. Furthermore, variation in techniques may lead to difficulties in comparison of structures of neurons reconstructed in different laboratories. (See also chapter 3 for a corresponding discussion.)

- *Completeness.* Some methods, such as Golgi stains, may not completely penetrate fine processes, giving an incomplete fill. Methods involving intracellular injection of small molecules (e.g., lucifer yellow, biocytin) are generally preferable because they result in more complete fills.
- *Shrinkage.* Before a neuron can be reconstructed, the neural tissue in which it is embedded must generally be fixed, a process whereby proteins are chemically cross-linked to immobilize them. Fixation results in varying amounts of tissue shrinkage depending on the exact method applied and a correction for this shrinkage must be determined or estimated. Some reconstructions will be corrected, while others will not. Shrinkages of 10%–20% are typical (Major et al. 1994; Mainen et al. 1996).
- *Wiggle.* Some fixation procedures, particularly those required for electron microscope (EM) processing, produce tissue distortion resulting in significant dendritic "wiggle." Failure to account for this tortuosity by sampling too few points during digital reconstruction will result in an underestimation of the dendritic length. In

some cases, a correction factor may be applied, the value of which will depend on the exact reconstruction technique (Major et al. 1994).

•• *Diameter estimation.* Estimation of small branch diameters can be problematic when these approach the resolution of the microscope. Systematic overestimation of small branch diameters is a strong possibility for ordinary light microscopy (Mainen et al. 1996). Although confocal microscopy offers better resolution of small processes, confocal reconstruction systems are still uncommon.

•• *Spine membrane.* The dendrites of pyramidal neurons are studded with dendritic spines that are typically not included in dendritic reconstructions. A simple method to account for these spines is to increase the membrane surface area to compensate for the additional spine membrane area, which can be as much as 50% (see Stratford et al. 1989; Rapp, Yarom, and Segev 1992; and Major et al. 1994). Measurements of spine densities for pyramidal neurons of several types are available (neocortex: Larkman 1991; CA1: Harris, Jensen, and Tsao 1992). Although EM measurements of spine dimensions are also available (neocortex: Peters and Kaiserman-Abramof 1970; CA1: Harris, Jensen, and Tsao 1992), these numbers may not apply to cells of other areas or different ages.

•• *Translation.* The data produced by digital reconstruction systems can usually be translated directly into a form suitable for incorporation into a simulation environment. The program NTSCable translates Eutectics, Nevin, and several other format files into NEURON code. Care must be taken with such automated translation programs because errors in reconstruction may be introduced by the translation. For example, there may be missing links between branches and trunks of dendrites. Representation of the soma is particularly problematic and often requires hand correction.

Passive Properties Along with the geometry, the passive membrane parameters complete a description of the cable properties of the neuron. These parameters are the membrane capacitance, C_m ("cm" in NEURON), the membrane resistivity, R_m ("1/g_pas" in NEURON), and the cytoplasmic or axial resistivity, R_i ("Ra" in NEURON). Although direct measurement of these parameters is difficult, experimental measurements combined with compartmental models provide indirect estimates (see chapter 2, this volume). Recent studies (Stratford et al. 1989; Spruston, Jaffe, and Johnston 1994; Major et al. 1994; Spruston and Stuart 1996, see also chapter 3, this volume) based on tight-seal whole-cell recordings (which are considered more accurate due to a smaller somatic "shunt") have generally arrived at estimates in the following ranges:

$$R_m = 20\text{--}100 \text{ k}\Omega \text{ cm}^2$$

$$C_m = 0.5\text{--}1.5 \text{ }\mu\text{F cm}^{-2}$$

$$R_i = 100\text{--}300 \text{ }\Omega \text{ cm}$$

In perhaps the most direct measurement to date, a study of neocortical pyramidal cells using double simultaneous whole-cell recordings from soma and apical dendrite and subsequent reconstruction and compartmental modeling (Spruston and Stuart 1996) found $R_i \approx 150 \text{ }\Omega \text{ cm}$.

The passive membrane properties are often taken to be uniform (e.g., Spruston and Johnston 1992; Major et al. 1994; Mainen et al. 1996). Although there is little or no direct support, the possibility that the passive parameters are nonuniform across the cell has been considered in several modeling studies (e.g., Fleshman, Segev, and Burke 1988; Rall et al. 1992; Rapp, Segev, and Yarom 1994; Stratford et al. 1989 and chapter 3, this volume). Because the leak conductance is thought to result from the one or more K^+ or mixed cation channels, possibly the ORK1 channel (Goldstein et al. 1996) that are active (and linear) near the resting potential (Theander, Fahraeus, and Grampp 1996), a nonuniform distribution of these channels could result in nonuniform R_m (Spruston and Stuart 1996). The case for nonuniformity of C_m or R_i is less clear. It is also worth noting that nonuniformity of spine density (Larkman 1991) can be considered to contribute to an effective nonuniformity of both C_m and R_m once the additional spine membrane area is added.

5.2.2 Active Channels

Chapter 4 describes active channel properties from voltage clamp data (also see Johnston and Wu 1995; Hille 1992). We focus here on issues particularly relevant to constraining models with spatially distributed active channels: estimating channel densities and localization of channel types.

Current through an ion channel can be described by an equation of the form

$$I(V_m, t) = \bar{g}p_o(V_m, t)(V_m - E), \quad (5.1)$$

where I is the total current, \bar{g} the maximum conductance, p_o a dynamic state variable representing the probability of channel opening or fraction of open channels (ranging from 0 to 1), V_m the membrane potential, and E the reversal potential of the channel in question. This equation assumes a linear or ohmic current-voltage relation. For most voltage-gated channels except those permeable primarily to Ca^{2+} , the ohmic approximation is reasonable. For Ca^{2+} channels, a more precise description of

the driving force is offered by the Goldman-Hodgkin-Katz equation (see chapter 6, this volume; Hille 1992).

The equations for channel activation, p_o , are generally based on the gate activation, m , and inactivation, h , formalism of Hodgkin and Huxley (1952; see chapter 4, this volume), although a more general description using kinetic equations is often used by biophysicists (see Destexhe, Mainen, and Sejnowski 1994). The same kinetic formalism can be used to describe ligand-gated ion channels (see chapter 1, this volume).

5.2.3 Temperature Dependence

Because many physiological studies are performed at room temperature (22°–25° C) rather than at physiological temperature (37°–40° C), it is often necessary to compensate for the impact of temperature on model parameters, in particular, channel kinetics and conductances. The usual strategy employed is to scale the rate constants by a temperature coefficient, Q_{10} (fractional rate increase per 10° C temperature increase). However, the kinetics of different channels are not necessarily equivalent in their temperature dependence, and even the activation and inactivation rates of a given channel may depend differently on temperature. For example, in a study of the temperature dependence of Na^+ currents (Schwarz and Eikhof 1987), the steady-state parameters were found to be insensitive to temperature (in accord with the usual assumption), while the activation and inactivation rates had Q_{10} values of 2.2 and 2.9, respectively. Temperature also may affect the conductance of ions through a channel and hence \bar{g} . For example, a Q_{10} of 1.4 was reported for the conductance of one type of calcium channel (Acerbo and Nobile 1994). Despite the significance of these findings for the construction of accurate kinetic models, voltage clamp experiments at physiological temperature and the necessary data on temperature dependence are still both scarce.

5.2.4 Density Estimation

A serious problem in models that include a variety of ion channels spread non-uniformly across the neuron is the huge number of parameters available to describe the channel densities. In the majority of detailed compartmental modeling studies (e.g., Lytton and Sejnowski 1991; Traub et al. 1991; Rhodes and Gray 1994; Jaeger, De Schutter, and Bower 1997), the channel densities have been considered as free parameters that are altered systematically (or haphazardly) until the desired physiological behavior is produced. Because the fitting of a highly complex model to experimental data is severely underconstrained, the need for independent estimates of channel density and localization is clearly critical. Although this information was in

the past essentially absent, through recent physiological and anatomical studies, many of these vitally needed parameters are now becoming available. Due to the importance of the topic, we will consider in some detail the process of incorporating channel density data into neural models.

While most compartmental models express channel density in terms of a maximal conductance, \bar{g} , this parameter cannot be measured experimentally, but rather must be calculated. Generally speaking, data on conductance densities are provided by two classes of experimental technique: anatomical and physiological, both of which have their advantages and limitations.

Anatomical Density Estimation Using techniques of molecular biology such as immunocytochemistry, anatomical techniques offer the possibility of superb specificity and resolution of subcellular channel localization. To resolve the distribution of ion channels, the channel must be bound by a probe molecule such as a specific toxin or, more commonly, a specific antibody. The primary probe is detected by attaching a secondary probe that is visible either fluorescently (typically a secondary antibody conjugated to a fluorophore) or by electron microscopy (typically a gold particle).

Given estimates of channel density, if the single-channel conductance is also known, then \bar{g} (pS/ μm^2) can simple be calculated from

$$\bar{g} = \gamma\rho, \quad (5.2)$$

where γ is the single-channel conductance (in pS) and ρ is the channel density (in channels/ μm^2).

Although molecular techniques make it possible to measure precisely and quantitatively the distribution of various channels, they have a number of limitations. First, most ion channels have several subunits, each with a variety of subtypes that can be recognized differentially by immunocytochemical probes. The properties of a given type of channel may vary widely depending on the precise subunit composition, yet in many cases the properties of these possible channel subtypes are not known. Second, most ion channels are subject to biochemical modulation, and therefore the true functional channel density will reflect not only the anatomical density but also the functional state of these channels. These limitations reinforce the value of physiological techniques.

Whole-Cell Recording Whole-cell and sharp-electrode voltage clamp recordings sample channel activity from both local and distant cell regions with a weighting that depends on the electrotonic structure of the cell and the frequency of the currents in question (White, Sekar, and Kay 1995; Zador, Agmon-Snir, and Segev 1995). Thus

estimating channel density in spatially complex neurons by whole-cell methods is at best a tricky proposition. Such estimates are typically only useful in cells lacking dendritic arbors, or those treated by enzymes to remove the dendrites (i.e., acutely dissociated cell cultures).

On the other hand, whole-cell and intracellular recordings can be used to qualitatively assay regional differences in channel densities by comparing currents in somatic and dendritic recordings (e.g., Andreasen and Lambert 1995) or by applying channel-blocking drugs in a local fashion to test for the presence of channels in particular region of the neuron (e.g., Huguenard, Hamill, and Prince 1989; Schwandt and Crill 1995; Lipowsky, Gillessen, and Alzheimer 1996; Colbert and Johnston 1996). The spatial resolution of these methods is clearly limited because (1) currents are measured over a range of electrotonic distances from the recording site; (2) electrotonically remote active channels cannot be voltage-clamped (White, Sekar, and Kay 1995); and (3) confirmation of the region of drug application is difficult. Nevertheless, local application of blocking drugs can provide invaluable qualitative tests of hypotheses regarding the function of channels in a compartment (Lipowsky, Gillessen, and Alzheimer 1996; Colbert and Johnston 1996).

Maximal conductance, \bar{g} , can be calculated from an isolated, voltage-clamped current if the driving force and fraction of open channels are known, using

$$\bar{g} = \frac{I}{p_o(V - E)A}, \quad (5.3)$$

where I is the maximal current amplitude, p_o the fraction of channels open at the maximal observed current, V the clamp potential, E the reversal potential of the channel, and A the area of membrane sampled. Note that if I is measured in pA, V in mV, and A in μm^2 then \bar{g} will be measured in $\text{nS}/\mu\text{m}^2$. Although it is commonly assumed that $p_o = 1$ (all channels open during the maximal observed current), for many channels, $p_o < 1$ due to channel inactivation. For example, in some models, peak open probability for the Na^+ channel is substantially less than one (Aldrich and Stevens 1987). This will lead to an underestimate of \bar{g} , which can be corrected by estimating the true p_o from a kinetic model of the channel in question. Note that the estimation of the area sample (A) may be the most difficult parameter in this equation to determine.

Single-Channel Recording Using patch clamp recordings in the outside-out or cell-attached configuration (Sakmann and Neher 1995b), it is possible to sample isolated single-channel currents from any location on a neuron that can be patched. This method, although more difficult, avoids many of the problems inherent in whole-cell voltage clamp experiments by confining the membrane examined to a small patch

drawn into the patch pipette. Thus both excellent voltage clamp and high spatial resolution are achieved. With the advent of visually guided patch techniques (reviewed in Stuart, Dodt, and Sakmann 1993), the repertoire of targets now includes larger dendritic processes (reviewed in Stuart and Spruston 1995) and proximal portions of the axon (Stuart and Sakmann 1994; Hausser et al. 1995; Colbert and Johnston 1996) as well as the soma.

Channel densities can be estimated directly from peak currents observed in patch recordings by eq. 5.3, or where single-channel currents can be observed, from

$$\rho = \frac{I}{p_o i A}, \quad (5.4)$$

where I is the peak current observed, i the single-channel current amplitude at the same holding potential, and A the estimated patch area. As described above, since $p_o \leq 1$, this is a lower bound on the actual number of channels and should be corrected using the actual p_o . In cases where single-channel currents cannot be resolved, fluctuation analysis (Sigworth and Zhou 1992) can be used to estimate the number of channels and single-channel conductance, providing \bar{g} by eq. 5.2.

There are two caveats to keep in mind when converting currents observed in patches to a \bar{g} parameter. First, patch areas are relatively difficult to estimate and most often measured indirectly. Area estimates may be fairly sensitive to errors in measurement of the pipette diameter and the amount of membrane drawn into the pipette. In one of the few systematic studies (Sakmann and Neher 1995a), membrane area in patches obtained with typical (2–3 M Ω) pipettes ranged from 5 μm^2 to 20 μm^2 . Extrapolation to smaller pipettes used in dendritic or axonal patches is difficult because of the high variance and lack of measurements of higher resistance pipettes. For example, in measurements of dendritic Na⁺ channel density with similar patch clamp techniques, Stuart and Sakmann (1994) estimated a 1.5 μm^2 patch area, while Magee and Johnston (1995a) estimated 3 μm^2 .

And second, in outside-out patches, channel activity may be increased or decreased relative to normal conditions due to perturbation of the cytoplasmic environment. For example, Na⁺ channels are regulated by protein kinase C, cAMP-dependent protein kinase, and phosphoprotein phosphatases (Murphy et al. 1993). Basal levels of cAMP-dependent kinase have been shown to produce significant functional inhibition of Na⁺ currents in intact cells (Li et al. 1992). The absence of endogenous kinase and phosphatase activity in the outside-out patch configuration might thus be expected to result in higher Na⁺ channel activity in outside-out patches compared to the intact cell.

Imaging Optical imaging of membrane potential or intracellular ion concentrations can also provide useful data on channel densities. The most successful method so far has been Ca^{2+} imaging. Because resting intracellular Ca^{2+} concentration is typically less than 100 nM, increases in Ca^{2+} concentration provide an excellent signal of voltage-dependent Ca^{2+} channel activity. Comparing the Ca^{2+} signal and time course of Ca^{2+} rises at different dendritic locations, it has been possible to localize the site of Ca^{2+} entry and thereby pinpoint the locations of ion channels selective for Ca^{2+} (see below). Recent advances, such as two-photon laser scanning microscopy (Denk et al. 1994), have opened up new avenues including the ability to observe Ca^{2+} entry in the dendrites of cortical neurons in vivo (Svoboda et al. 1997). However, although Ca^{2+} enters through several varieties of voltage-dependent calcium channel (see below), it also enters through the NMDA-type glutamate receptor (see chapter 1, this volume) and can also be released from intracellular stores (reviewed in Pozzan et al. 1994). Thus the interpretation of Ca^{2+} imaging data can be tricky (some of the issues involved are discussed in more detail in chapter 6, this volume).

Na^+ Imaging Na^+ -sensitive dyes such as Na^+ -green are available and have been used to localize Na^+ channels (e.g., Jaffe et al. 1992; Tsubokawa and Ross 1996; and see below). Because internal Na^+ concentration is fairly high, the signal-to-noise of these dyes is low. Nonetheless, it has been possible to show, for example, that the axon hillock region of Purkinje cells in the cerebellum are a "hot spot" for Na^+ entry, suggesting a higher density of Na^+ channels there than in the soma and dendritic regions (Lasser-Ross and Ross 1992).

Membrane Potential Imaging Voltage-sensitive dyes, used for some time to measure events in small processes of cultured neurons (Grinvald, Ross, and Farber 1981), have recently been used to examine passive properties (Fromherz and Muller 1994) and spike initiation (Zečević 1996). Newly developed dyes (Kogan et al. 1995; Antić and Zečević 1995; Gonzalez and Tsien 1995) promise better signal-to-noise and hence better resolution.

5.2.5 Channel Types

This section briefly reviews the chief players in active dendritic processing, the voltage-gated ion channels, with particular attention to their subcellular localization in pyramidal neurons (table 5.1). We generally combine data from hippocampal and neocortical pyramidal neurons with data from other cell types that may be particularly applicable. Let us start with some general comments on these data (axonal currents are considered separately in section 5.2.6).

Table 5.1
Table of currents discussed in this chapter

Current	Channel	γ (pS)	Activation	τ_{inact} (ms)
I_{Na}	Na ⁺ (Na)	15–20	$\uparrow = V_{\theta}$	1
I_{Na_p}	Na ⁺ (Na)	15–20	$\uparrow < V_{\theta}$	—
I_T	Ca ²⁺ (LVA)	7–10	$\uparrow \approx V_{\theta}$	50
I_{Ca-NR}	Ca ²⁺ (HVAm)	14–18	$\uparrow > V_{\theta}$	100
I_{Ca-L}	Ca ²⁺ (HVA1)	25–30	$\uparrow > V_{\theta}$	—
I_A	K ⁺ (Kv)	5–10	$\uparrow \approx V_{\theta}$	5–25
I_{Kd}	K ⁺ (Kv)	5–10	$\uparrow > V_{\theta}$	—
I_C	K ⁺ (BK)	?100	\uparrow Ca ²⁺ (L)	—
I_M	K ⁺ (cag?)	small	$\uparrow < V_{\theta}$	—
sI_{AHP}	K ⁺ (?)	?	\uparrow Ca ²⁺ (R)	—
I_{AHP}	K ⁺ (SK)	5–20	\uparrow Ca ²⁺ (N)	—
I_H	K ⁺ /Na ⁺ (Kir?)	?	$\downarrow < V_{\theta}$	—
I_{IR}	K ⁺ /Na ⁺ (Kir)	?	$\downarrow < V_{\theta}$	—

Where it is known, the channel underlying the observed currents is given (? indicates that the channel is still unknown or speculative). The single-channel conductance (γ) is useful for converting between channel densities and conductance densities. The entries in the "Activation" column describe whether the channel is activated (\uparrow) or inactivated (\downarrow) by Ca²⁺ or depolarization. The parenthetical letters refer to the subtype of Ca²⁺ channel believed to be associated with different Ca²⁺-activated K⁺ currents. The voltage range of activation relative to action potential threshold (V_{θ}) is also given. The rightmost column gives the approximate time constant of inactivation (if present). References are given in the text.

General Observations

- A wide variety of voltage-dependent channels are present in dendritic membranes, and include all major families of sodium, potassium, and calcium channels.
- Some channel subtypes are confined to dendritic, somatic, or axonal compartments (e.g., Westenbroek, Merrick, and Catterall 1989; Hell et al. 1993; Sheng et al. 1992); this may be primarily for differential modulation because functional properties of the different subtypes are often similar.
- Some channel types, notably, certain Ca²⁺ and Ca²⁺-dependent K⁺ subtypes (Sah 1995), may coassociate, forming functionally specific units.
- Some voltage-gated channels show microscale dendritic clustering, including exclusion or enrichment in dendritic spines (e.g., Ahlijanian, and Catterall Westenbroek, 1990; Turner et al. 1994); the electrophysiological impact of this clustering is not well known.
- Above the microscale, changes in channel density appear to be relatively gradual through the dendrites and soma, while possibly more abrupt in the axon.

- Voltage-gated channel densities in dendrites estimated by patch clamp recordings are generally within a fairly narrow range (<10 channels/ μm^2 ; see figure 5.1), although density estimates by various molecular methods for axonal Na^+ channels and synaptic receptors can be extremely high ($>1,000$ channels/ μm^2).

Sodium Channels Electrophysiological and modeling studies have differentiated between a fast or transient Na^+ current, I_{Na} , and a persistent Na^+ current, I_{Na_p} (reviewed in Crill 1996). The transient current mediates the fast action potential, while the persistent current activates below threshold, may boost synaptic currents in dendrites (Stuart and Sakmann 1995; Schwindt and Crill 1995; Lipowsky, Gillessen, and Alzheimer 1996), and contribute to bursting (Franceschetti et al. 1995) and subthreshold oscillations (Gutfreund, Yarom, and Segev 1995) in neocortical neurons.

KINETICS Single-channel recordings indicate that the fast and persistent Na^+ currents are mediated by the same type of Na^+ channel, entering either a rapidly or a slowly inactivating mode (Kirsch and Brown 1989; Alzheimer, Schwindt, and Crill 1993; Brown, Schwindt, and Crill 1996; Magee and Johnston 1995a). Because complex gating is not readily incorporated into the Hodgkin-Huxley framework, all models to date have treated I_{Na} and I_{Na_p} as two distinct currents. A full Markov model of the Na^+ channel (e.g., Vandenberg and Bezanilla 1991; Destexhe, Mainen, and Sejnowski 1994) would be desirable. I_{Na} kinetics can be difficult to determine because the currents are large and fast and therefore hard to voltage-clamp without introducing artifacts (White, Sekar, and Kay 1995). I_{Na} kinetics described by Huguenard and colleagues (Huguenard, Hamill, and Prince 1988; Hamill, Huguenard, and Prince 1991; Mainen et al. 1995) in dissociated neocortical pyramidal cells are very similar to those observed in rat brain Na^+ channels expressed in oocytes (Stühmer et al. 1987), and those measured in rat and human neocortex (Cummins, Xia, and Haddad 1994). The steepness of the activation curve (9 mV/ e -fold) is about half as steep as that used in an I_{Na} model introduced by Traub and colleagues (1991, 1994) and used in a number of other recent models. The kinetics of I_{Na_p} were described by French et al. (1990) in hippocampal neurons, and their data has formed the basis for the current used in most recent models (e.g., De Schutter and Bower 1994a; Gutfreund, Yarom, and Segev 1995; Lipowsky, Gillessen, and Alzheimer 1996). The model includes an activation variable only.

DISTRIBUTION Assuming that I_{Na} and I_{Na_p} derive from the same underlying channel, the distributions of their currents should be the same, although the magnitude of I_{Na_p} is approximately 1% of the transient Na^+ current (Crill 1996). However, it is possible

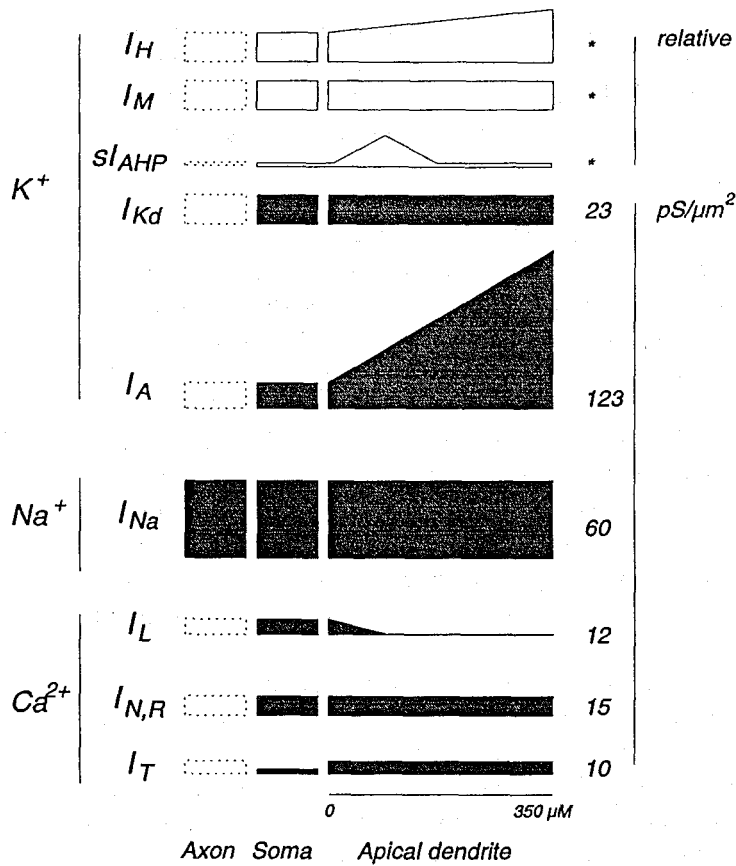


Figure 5.1

Schematic diagram of conductance densities (\bar{g}) in pyramidal cells estimated by direct, cell-attached patch recordings (shaded: I_{Kd} , I_A , I_{Na} , I_{Ca}) or inferred from combined modeling and electrophysiology studies (white boxes: I_H , I_M , sI_{AHP}). Dotted lines: not measured. Conductance densities are those reported by the authors or calculated from reported channel densities, using eq. 5.2. The apical dendritic distance scale is approximately correct, but the somatic and axonal distances are not to scale. Numbers on the right indicate the maximum average peak conductance density for each channel. I_H , I_M from Hutcheon et al. 1996; sI_{AHP} from Sah and Bekkers 1996; I_{Kd} , I_A from Hoffman Magee, and Johnston 1996; Hoffman et al. 1997; I_{Na} from Stuart and Sakmann 1994; Magee and Johnston 1995a; Colbert and Johnston 1996; I_L , $I_{N,R}$, from Magee and Johnston 1995a.

that the ratio of I_{Na} to I_{Na_p} differs across subtypes of Na^+ channel, which show a nonuniform subcellular distribution (Westenbroek, Merrick, and Catterall 1989).

Single-channel dendritic recordings have allowed direct measurements of dendritic Na^+ channels on the apical dendrite of neocortical and hippocampal pyramidal neurons (Huguenard, Hamill, and Prince 1989; Stuart and Sakmann 1994; Spruston, Jonas, and Sakmann 1995; Magee and Johnston 1995a, 199b). These recordings indicate that the density of Na^+ channels on somatic and dendritic membrane is similar, in the range of 30–60 pS/ μm^2 . Magee and Johnston (1995a) have provided evidence that the developmental increase in Na^+ channel density (Huguenard, Hamill, and Prince 1988) may proceed more rapidly in the soma than dendrites, such that in juvenile animals (<4 weeks) the apical dendrite has a lower density than the soma. Although these recordings definitively establish the presence of functional dendritic Na^+ channels, their uniformity and their density on small-diameter branches and spines are not yet determined and may require the use of molecular anatomical techniques. One study of this kind (Turner et al. 1994) found Na^+ channels throughout the apical and basal dendrites, in pyramidal cells of the electrosensory lateral line lobe of the weakly electric fish. Significantly, the labeling occurred in discrete patches rather than uniformly and was absent from the dendritic spines and subsynaptic membrane.

A possible difference between neocortical layer-5 and hippocampal CA1 pyramidal neurons is the spatial extent of Na^+ channels in the apical dendrite. Imaging of intracellular Na^+ ions in hippocampal pyramidal cell dendrites showed that Na^+ entry was confined to the proximal dendritic regions (Jaffe et al. 1992). Likewise, in CA1 neurons Ca^{2+} elevations produced by antidromically propagating action potentials are substantially greater in proximal than distal dendrites (Jaffe et al. 1992), even though a more uniform pattern of Ca^{2+} entry can be seen when K^+ channels are blocked (Jaffe et al. 1992). In contrast, Ca^{2+} elevations in layer-5 neurons are high throughout the dendritic arbor (Schiller, Helmchen, and Sakmann 1995), suggesting that antidromically propagating spikes can fully invade the dendrites in slice preparations, although the extent of the invasion may be regulated in vivo (Svoboda et al. 1997). These observations suggest that while Na^+ channel density in distal dendrites may be lower than in more proximal regions in CA1 pyramidal cells, this gradient may not be as large in neocortical pyramidal cells, although differences in experimental methods and animal age may also contribute to the differences in these findings.

Calcium Channels Voltage-dependent Ca^{2+} channels (VDCCs) appear to be present throughout the dendrites of pyramidal cells. Ca^{2+} entering through these VDCCs can contribute to a wide variety of biochemical cascades triggered by Ca^{2+} , includ-

ing neurotransmitter release and synaptic plasticity. Ca^{2+} entry through VDCCs activates Ca^{2+} -dependent K^+ channels (see below), which leads to hyperpolarization that tends to limit cell firing. Under some conditions, Ca^{2+} channels participate in regenerative bursting or plateau potentials (Wong, Prince, and Basbaum 1979; Kim and Connors 1993; Yuste et al. 1994; Hirsch, Alonso, and Reid 1995).

SUBTYPES There are two main classes of VDCCs; low-voltage- and high-voltage-activated (LVA and HVA). The LVA class corresponds to I_T (T-current) which is activated in the subthreshold voltage range. Possible functions suggested for I_T include generation of low-threshold spikes that lead to burst firing, promotion of intrinsic oscillatory behavior, boosting of calcium entry for hyperpolarized cells, and synaptic potentiation (reviewed in Huguenard 1996). The HVA class includes L-, N-, P-, Q-, and R-type currents (Tsien et al. 1988; Randall and Tsien 1995). While the different HVA Ca^{2+} channels vary in their distribution, pharmacological sensitivity, modulation, and inactivation properties, all are activated in similar superthreshold voltage ranges and may produce currents of essentially identical kinetics during physiological activity (Brown, Schwindt, and Crill 1993). As a consequence, in most models of pyramidal neurons, a single channel type (often simple called I_{Ca}) has been used to represent all classes of HVA channel (e.g., Traub et al. 1991, 1994; Reuveni et al. 1993; Warman, Durand, and Yuen 1994; Rhodes and Gray 1994; Mainen and Sejnowski 1996), although Ca^{2+} imaging experiments suggest that N- (slowly inactivating) and L-type (noninactivating) currents can be distinguished in more detailed models (Jaffe and Brown 1994; Migliore, Alicata, and Ayala 1995).

DISTRIBUTION The range of data on dendritic VDCCs in hippocampal and neocortical pyramidal neurons is growing rapidly. Ca^{2+} imaging studies have shown that VDCCs are located throughout the dendritic arbor (Regehr, Connor, and Tank 1989; Miyakawa et al. 1992; Jaffe et al. 1992; Schiller, Helmchen, and Sakmann 1995) including dendritic spines (Jaffe, Fisher, and Brown 1994; Segal 1995; Denk et al. 1996), as well as in the axon initial segment (Schiller, Helmchen, and Sakmann 1995) and, of course, presynaptic terminals. Localized calcium influx produced by subthreshold synaptic events (Markram and Sakmann 1994; Magee et al. 1995) occurs through LVA channels that can be activated by such stimuli (Magee and Johnston 1995b). In contrast, HVA channels are activated by backpropagating Na^+ action potentials (Schiller, Helmchen, and Sakmann 1995; Spruston, Jonas, and Sakmann 1995a; Markram, Helm, and Sakmann 1995; Helmchen, Imoto, and Sakmann 1996; Svoboda et al. 1997; Magee and Johnston 1997; Markram et al. 1997), dendritic Ca^{2+} bursting (Yuste et al. 1994) or by repetitive trains of synaptic stimuli (Miyakawa et al. 1992).

Pharmacological dissection of the contribution of various VDCCs to dendritic Ca^{2+} influx suggests that in CA1 neurons, I_T (LVA Ca^{2+} channels) are preferentially located in more distal dendrites while HVA Ca^{2+} channels are more concentrated in the soma and proximal dendrites (Christie et al. 1995). I_T is also concentrated in the distal dendrites of thalamic neurons (Destexhe et al. 1996). Single-channel patch recordings in apical dendrites of pyramidal cells support these findings (Magee and Johnston 1995a). In CA1 neurons the overall combined density of dendritic Ca^{2+} channels is about 50%–75% that of voltage-gated Na^+ channels (Magee and Johnston 1995a).

Immunocytochemical methods yield findings generally consistent with the physiological data, suggesting that VDCCs are clustered rather than uniformly distributed in the dendrites (Jones, Kunze, and Angelides 1989), with L-type channels localized to the base of major dendrites as well as the soma (Westenbroek, Ahljianian, and Catterall 1990). Similar methods show N-type channels are present in the soma, dendrites, and a subset of dendritic spines (Mills et al. 1994). Further dissection of the subcellular localization of various VDCC subunits (Hell et al. 1993; Westenbroek et al. 1995; Yokoyama et al. 1995; Sakurai et al. 1996) is providing a basis for an even finer-grained analysis of the subcellular distribution of VDCCs and other channels. Models that take subcellular localization into account could help in exploring the functional consequences of VDCC clusters.

Potassium Channels K^+ channels are a large and diverse group (see reviews by Storm 1990; Christie 1995; Sah 1996). Functionally, the K^+ currents can be divided into three primary groups according to function: (1) spike repolarization, I_A , I_{Kd} , I_C ; (2) spike frequency adaptation, I_M , I_{AHP} , sI_{AHP} ; and (3) anomalous rectification, I_H , I_{IR} . While several other types of K^+ current have been described, including Na^+ -dependent K^+ currents (Schwindt, Spain, and Crill 1989) and several very slow voltage-gated currents such as I_D (Storm 1988), these have not yet been incorporated into models.

FAST SPIKE REPOLARIZATION In pyramidal neurons, action potentials are repolarized by both voltage- and Ca^{2+} -dependent K^+ currents (Storm 1987). The former are members of the large and diverse Kv family of voltage-gated K^+ channels (Christie 1995), and include a class of inactivating currents, I_A , as well as noninactivating or delayed-rectifier currents, I_{Kd} . In addition to these voltage-gated currents, I_C , which is activated by both voltage and Ca^{2+} , also contributes significantly to spike repolarization (Lancaster and Nicoll 1987; Storm 1987). I_C is mediated by the large-conductance (BK) class of K^+ channel (Christie 1995).

Models for I_A are given by Banks, Haberly, and Jackson (1996, based on recordings from pyriform cortical neurons) and Hoffman et al. (1997, based on recordings in hippocampal CA1 neurons). A model for I_{Kd} is given by Mainen et al. (1996), based on data from neocortical neurons described in Hamill, Huguenard, and Prince (1991). Although the calcium and voltage dependence of I_C have been characterized in nonneuronal cells (Barrett, Magleby, and Pallotta 1982), kinetic descriptions from neocortical or hippocampal pyramidal neurons are not yet available. Consequently, models of I_C in these neurons are still based on data culled from diverse preparations and can be considered somewhat less than canonical. A model of I_C based on studies in muscle cells by Moczydlowski and Latorre (1983) is included in NEURON; another, based on data from bullfrog sympathetic ganglia, is given in chapter 4. Models of I_C in pyramidal cells based on modifications of these and other data are given by Traub et al. (1991); Lytton and Sejnowski (1991); De Schutter and Bower (1994a); and Warman, Durand, and Yuen (1994).

Owing to the relatively slow repolarization of dendritic action potentials (e.g., Wong, Prince, and Basbaum 1979; Turner et al. 1991; Stuart and Sakmann 1994), modeling studies have assumed that the density of fast K^+ currents is higher in the soma and proximal dendrites (Mainen et al. 1995; Rapp, Yarom, and Segev 1996; Traub et al. 1994). There is however, no direct physiological or molecular evidence for this assumption, and some recent evidence argues for higher densities of dendritic K^+ channels farther from the soma (Hoffman, Magee, and Johnston 1996; Hoffman et al. 1997).

Different subtypes of Kv channels show highly specific patterns of cell type specific expression and subcellular localization (Sheng et al. 1992, 1994; Wang et al. 1994; Maletic-Savatic, Lenn, and Trimmer 1995; Weiser et al. 1995). These complex and diverse patterns clearly provide a rich substrate for possible differential regulation, a subject which is just starting to be unraveled. To the extent that dendritic K^+ channels are important for the transformation of synaptic currents into spike firing patterns, it should be expected that even among various subclasses of pyramidal cells, variability in K^+ channel expression may lead to heterogeneity in cellular integration properties. In the hippocampus, I_{Kd} -mediating subtypes (Kv1.5, Kv2.1, and Kv2.2) are expressed in proximal dendrites, while I_A -mediating subtypes (Kv1.4 and Kv4.2) are present in the distal dendrites of a subpopulation of neurons (Maletic-Savatic, Lenn, and Trimmer 1995). Another I_A subtype (Kv1.2) is also specifically expressed in the dendrites of neocortical and hippocampal pyramidal cells (Sheng et al. 1994).

Channels with properties corresponding to I_A , I_{Kd} , and I_C have been described in dendritic patches from CA1 pyramidal neurons (Hoffman, Magee, and Johnston

1996; Hoffman et al. 1997). The channel densities measured by this technique show a pattern of K^+ channel segregation consistent with the anatomical data: relatively constant I_{Kd} and I_A increasing in the dendrites with distance from the soma (Hoffman et al. 1997; discussed further in section 5.3).

SPIKE FREQUENCY ADAPTATION Like spike repolarization, spike frequency adaptation is mediated by both voltage- and Ca^{2+} -dependent K^+ channels (Madison and Nicoll 1984). These channels are essential to determining the relative sensitivity of a neuron to transient versus sustained inputs and limiting the response to large inputs, enabling a wide dynamic range of synaptic currents to be mapped to physiological firing frequencies (Mainen 1996; Tang, Bartels, and Sejnowski 1997). Electrophysiologically, the currents from these channels can also be seen as afterhyperpolarizations (AHPs) following a spike train (Madison and Nicoll 1984; Schwindt et al. 1988; Storm 1990) or sometimes a single spike or subthreshold event (e.g., Stuart and Sakmann 1995; Lipowsky, Gillessen, and Alzheimer 1996). Whereas the fast K^+ currents I_A , I_{Kd} and I_C contribute to what is known as the fast AHP, the much slower K^+ currents give rise to the medium AHP (I_M and I_{AHP}) or the slow AHP (sI_{AHP} ; Schwindt et al. 1988; Storm 1989; Sah 1996).

I_M is a slow, muscarine-sensitive, voltage-dependent K^+ current (Adams, Brown, and Constanti 1982) present in neocortical and hippocampal pyramidal neurons (Halliwell 1986; Schwindt et al. 1988; Storm 1989). I_M activates near threshold and does not inactivate (Adams, Brown, and Constanti 1982) and is one of several currents that contribute to the mAHP (Storm 1989). In addition to its role in modulating firing sensitivity and adaptation, I_M is partially activated at the resting membrane potential and, combined with I_{Na_p} , can give rise to subthreshold oscillations in cortical pyramidal neurons (Alonso and Klink 1993; Gutfreund, Yarom, and Segev 1995). The kinetics of I_M ($\tau \approx 30$ – 50 msec) are intermediate between the fast K^+ currents described above and the Ca^{2+} -dependent K^+ currents (I_{AHP} and sI_{AHP}). The channels underlying I_M are not yet firmly established, but may belong to a family of proteins (*eag*) related to the Kv family (Christie 1995). A model of an I_M current based on data from neocortical neurons is given by Gutfreund, Yarom, and Segev (1995).

There are at least two types of slow Ca^{2+} -dependent K^+ currents that contribute to spike frequency adaptation: I_{AHP} (or mI_{AHP}) and sI_{AHP} (Madison and Nicoll 1984; Lancaster and Adams 1986; Schwindt et al. 1988; Schwindt, Spain, and Crill 1992; Sah 1996). These two types of currents, which have often been confused, can be distinguished by their time course and pharmacological profiles. The faster I_{AHP} (1–5 msec rise, 100–200 msec decay) is believed to correspond to the SK class of K^+

channel (Sah 1996), while the channel underlying the slower sI_{AHP} (>100 msec rise, >1 sec decay) is not known at present, but may be a subtype of SK channel (Sah 1996). Because the biophysical mechanisms underlying these currents are poorly understood, the existing models of I_{AHP}/sI_{AHP} are still quite speculative and are based on a mixture of data from different neuronal types (examples are found in Traub et al. 1991; Warman, Durand, and Yuen 1994).

There is evidence that Ca^{2+} ions rather than channel kinetics determine the time courses of these currents, as well as I_C (Lancaster and Zucker 1994; Sah 1993). It is not precisely known how different K^+ channel types would access Ca^{2+} signals with the necessary differences in time course, but the molecular coupling of the Ca^{2+} -dependent K^+ channels and the Ca^{2+} channels that are the source of their activation signal is thought to play a crucial role. In rat sympathetic neurons, it has been shown that Ca^{2+} entry via L-type channels selectively activates BK K^+ channels (producing the action potential–repolarizing I_C), while Ca^{2+} entry via N-type channels selectively activates SK K^+ channels (producing I_{AHP}), and Ca^{2+} entry via R-type Ca^{2+} channels activates Ca^{2+} release from intracellular stores (producing sI_{AHP} ; Davies, Ireland, and McLachlan 1996). A similar story might hold in pyramidal neurons. Conventional compartmental models have generally simulated one or more pools of intracellular Ca^{2+} that directly gate the K^+ channel (e.g., Warman, Durand, and Yuen 1994; Migliore, Alicata, and Ayala 1995). Ca^{2+} handling is treated in detail in chapter 6, this volume. An interesting avenue to explore would be models in which specific K^+ channel types are coupled to specific Ca^{2+} channel types and Ca^{2+} stores.

Relatively little is known about the density or distribution of slow voltage-dependent K^+ currents in pyramidal neurons, though a number studies have implicated a dendritic localization of slow K^+ currents. First, insofar as I_M is responsible for subthreshold oscillations, dendritic recordings indicate that it must be present in the apical dendrites in order to reproduce the observed resonance properties of neocortical neurons (Hutcheon et al. 1996). Dendritic recordings from CA1 neurons have also suggested the presence of a slow dendritic Ca^{2+} -dependent K^+ current (Andreasen and Lambert 1995). In an interesting combined modeling and electrophysiological study, Sah and Bekkers (1996) argued that sI_{AHP} must be localized to the proximal apical dendrite (within $\approx 200 \mu\text{m}$) in order to reproduce the interaction of the current with inhibitory postsynaptic potentials (IPSPs) and the observed offset of the current under voltage clamp. Whether their findings reflect localization of the K^+ channels or of the Ca^{2+} signals activating these channels has not been determined.

INWARD RECTIFICATION The final class of K^+ currents (which includes mixed cation currents), are tonically active at subthreshold membrane potentials, are activated by *hyperpolarization* rather than depolarization, and do not inactivate. The slow mixed-cation (Na^+/K^+) current I_H (also sometimes known as I_Q) underlies slow oscillatory behavior in several cell types and has been shown to be present in neocortical pyramidal neurons and to contribute to subthreshold membrane resonance (Spain, Schwandt, and Crill 1990; Perkins and Wong 1995; Hutcheon, Miura, and Pail 1996a, 1996b). The anomalous rectifying K^+ current, I_{IR} has similar properties to I_H , but with much faster kinetics (Constanti and Galvan 1983; Sutor and Hablitz 1993).

The inwardly rectifying currents belong to a relatively large class of K^+ channels, known logically as the "inward rectifier family" (Kir; reviewed in Doupnik, Davidson, and Lester 1995). Not much is known about the subcellular distribution of these channels. Based on dendritic recordings and modeling of subthreshold oscillations in neocortical pyramidal neurons, Hutcheon, Miura, and Pail (1996a) argued for the presence of I_H in the dendrites (as well as the soma). Because the inward rectifiers are tonically active at resting membrane potentials, a nonuniform distribution of these channels would result in an effectively nonuniform membrane resistance. The possibility of dendritic membrane enriched in I_H or I_{IR} could complicate substantially the interpretation of passive membrane models. Based on a study combining dual somatic/dendritic recordings and compartmental modeling, Spruston and Stuart (1996) have suggested that I_H may indeed be concentrated in the apical dendrite.

5.2.6 Axonal Structure and Function

In a passive compartmental model, the axon contributes very little to dendritic or somatic behavior because its fine caliber and electrical isolation from the remainder of the cell produce little passive load (Rall et al. 1992). In models with active properties, however, the axon (or at least its proximal segments) may contribute substantially to the behavior of the neuron due to the contribution of voltage-gated Na^+ channels that make the axon the site of action potential initiation (Coombs, Curtis, and Eccles 1957a; Stuart and Sakmann 1994; Spruston, 1995; Colbert and Johnston 1996). Although the majority of published compartmental models omit the axon, several recent models of pyramidal cells have incorporated axonal anatomy as an essential component (e.g., Traub et al. 1994; Mainen et al. 1995; Rapp, Yarom, and Segev 1996).

Anatomy In pyramidal cells, the axon arises from the soma or in some cases from a basal dendrite. The transitional region where the axon meets the soma is known as

the "axon hillock." The *initial segment* of the axon is an ultrastructurally specialized region that generally extends to the first myelinated segment and is the target of about 20–50 axoaxonic inhibitory synapses (Peters, Proskauer, and Kaiserman-Abramof 1968; Jones and Powell 1969; Fariñas and DeFelipe 1991) made by a special class of GABA-ergic inhibitory interneurons called "chandelier cells" (Somogyi, Freund, and Cowey 1982).

In pyramidal neurons of the neocortex and hippocampus, the length of the initial segment ranges from about 20 μm to 50 μm (Sloper and Powell 1978; Somogyi, Freund, and Cowey 1982; Fariñas and DeFelipe 1991; Colbert and Johnston 1996) with an average diameter in the range of 1–2.5 μm (Westrum 1970; Fariñas and DeFelipe 1991). There is generally a 2- to 4-fold taper from the hillock to the distal end (Fariñas and DeFelipe 1991).

In myelinated axons, the myelin sheath begins at the end of the initial segment and is interrupted regularly by the nodes of Ranvier. In the terminal arbors of cat cortical axons, an internodal length of around 100 μm is typical (Waxman and Melker 1971; Deschênes and Landry 1980a), but systematic studies of internodal lengths of proximal axonal arbors are not available. The myelinated segments are thicker than the initial segment or nodes of Ranvier (Palay et al. 1968), with diameters in the range of 0.5–2 μm (Haug 1968). It is also important to note that myelination is only partially developed in the juvenile rats used in many electrophysiological studies.

Sodium Channels The propagation of nerve impulses in myelinated axons depends critically on localization of Na^+ channels to the nodes of Ranvier (Black, Kocsis, and Waxman 1990). Similarly, localization of Na^+ channels to the axon initial segment (Angelides et al. 1988; Kobayashi et al. 1992) has been proposed to contribute to the role of this structure as the site of action potential initiation (Coombs, Curtis, and Eccles 1957a; Dodge and Cooley 1973; Mainen et al. 1995; Rapp, Yarom, and Segev 1996). A primary distinguishing feature of both the initial segment and the nodes of Ranvier is the presence of an electron-dense undercoating (Peters, Proskauer, and Kaiserman-Abramof 1968), which has long been thought to be related to electrical conduction (Peters, Proskauer, and Kaisermann-Abramof 1968; Palay et al. 1968), presumably reflecting to an elevated density of Na^+ channels. The existence of structural barriers to diffusion of Na^+ channels between the axon hillock and soma (Srinivasan et al. 1988; Kobayashi et al. 1992) could provide the molecular basis for the trapping of channels in the initial segment. Conventional estimates of nodal Na^+ channel density are 1,000–2,000 channels/ μm^2 , compared with a 30-fold lower density in internodal regions (Black, Kocsis, and Waxman

1990; Waxman and Ritchie 1993). But is there a similar difference in channel density between soma and initial segment?

Measurements with fluorescent toxin-binding studies (Angelides et al. 1988) have shown up to 30-fold higher Na^+ channel density in the initial segment compared to the soma in cultured spinal cord neurons, consistent with the analogy to node and internode, although lower differences (<10-fold) were found in cortical neurons (Angelides et al. 1988) and retinal ganglion cells (Wollner and Catterall 1986). Moreover, using direct patch clamp recordings from the initial segments of subicular pyramidal cells, Colbert and Johnston (1996) found *no difference* between somatic and initial segment densities. Because the Na^+ channels of the initial segment may be clustered (Angelides et al. 1988; Turner et al. 1994), it is possible that sampling problems hampered the patch clamp estimates. On the other hand, Colbert and Johnston (1996) also found no evidence for a substantially lower threshold at the initial segment compared to the soma, throwing considerable doubt on the applicability of the classical model to action potential initiation in pyramidal cells (see also below).

Other Properties Because of their small diameters, central axons are very difficult to measure electrophysiologically. There is consequently very little such data on axonal specializations of voltage-dependent channels or other electrical properties. As for dendrites, all major channel types are likely to be found in axonal membranes, albeit perhaps different subtypes at different densities. The presence of a variety of Ca^{2+} channels in axon terminals responsible for neurotransmitter release is well documented (reviewed in Reuter 1996). Various members of the Kv family of K^+ channels (corresponding to I_A and I_{Kd}) have been localized to axons in immunocytochemical studies.

Myelinated axon segments generally have very low capacitance (Black, Kocsis, and Waxman 1990; Hille 1992), for example, $0.04 \mu\text{F}/\text{cm}^2$ (Graham and Redman 1994). While there may be very little leak current or other channels associated with myelinated axonal segments, the resistance of the nodes is believed in some cases to be substantially lower than even that of somatodendritic membrane (Blight 1985; Black, Kocsis, and Waxman 1990), for example, $50 \Omega \text{cm}^2$ (Graham and Redman 1994). This lower resistance could help to repolarize the membrane following an action potential in the absence of a delayed rectifier current, although various K^+ channels are known to be present in axons (Sheng et al. 1992, 1994; Wang et al. 1994; Maletic-Savatic, Lenn, and Trimmer 1995; Weiser et al. 1995). In addition, several recent modeling studies have used lower axonal than dendritic axial resistivity, for example, $70\text{--}100 \Omega \text{cm}$ versus $200\text{--}300 \Omega \text{cm}$ (Traub et al. 1994; Rapp, Yarom, and

Segev 1996; Migliore 1996), although there is little experimental evidence to support a disparity.

Propagation Compared to dendritic processing, the subject of computation in the axons of pyramidal neurons has received relatively little attention (see reviews in Waxman 1975; Wall 1995). Three main classes of computation have been examined: (1) history-dependent spatiotemporal filtering of impulses (Chung, Raymond, and Lettvin 1970; Deschênes and Landry 1980b; Lüscher and Shiner 1990); (2) temporal delay processing (Manor, Koch, and Segev 1991); and (3) presynaptic inhibition of impulse conduction (Segev 1990; Graham and Redman 1994). These studies have been based on relatively simple models of action potential propagation (i.e., based on classical Hodgkin-Huxley Na^+ and K^+ currents), although evidence suggests that most of the channels contributing to the complexity of dendritic behavior are also present in axons. The potential impact of non-Hodgkin-Huxley channels on action potential conduction in axonal arbors (Lüscher et al. 1994b, 1994a) certainly bears further examination in compartmental models.

5.2.7 Exploring Parameters

From the data reviewed above, it is apparent that the practice of treating dendritic channel densities as free, unconstrained parameters is rapidly becoming untenable. It is nevertheless true that any model of a spatially extended neuron with active conductances will retain some degree of flexibility in assigning channel densities. Heterogeneity among cell subtypes and over developmental ages as well as variability across individual cells means that the idea of a canonical channel distribution will at best be a rough sketch. "Tuning" channel densities to fit a set of electrophysiological data will therefore be necessary. Indeed, this is considered to be the most arduous task in constructing a compartmental model and raises an interesting theoretical issue as to how each neuron determines and regulates these densities. One intriguing possibility is that local information in the time-varying membrane potentials and ion concentrations may control the local densities of particular channel types through up- and down-regulation as well as other biophysical mechanisms (Bell 1992; Siegel, Marder, and Abbot 1994 and chapter 10, this volume). The immediate concern of most modelers, however, is to find some way to constrain the parameters by matching simulations to experimental recordings.

In most studies, channel densities (and other parameters) are tuned by hand; that is, by trial and error, starting with plausible values for the parameters and changing them in some systematic way (e.g., Lytton and Sejnowski 1991; Traub et al. 1991, 1994; Rhodes and Gray 1994; Migliore, Alicata, and Ayala 1995; Mainen and

Sejnowski 1996). Although, in some cases, individual parameters may be directly related to specific electrophysiological variables, the correspondence is seldom simple: most behaviors are the net result of the interaction of multiple currents with the electrotonic structure of the neuron (Mainen and Sejnowski 1996). There is very little explicit description in the modeling literature about how the process of parameter tuning is carried out. In the best cases, a particular final set of channel densities is loosely justified in terms of direct measurements and their effects on net electrophysiological behavior (e.g., Traub and Llinás 1979, Traub 1982; Traub et al. 1985, 1991; Quadroni and Knöpfel 1994). A promising approach in this regard is the use of a combination of *in vitro* and *in vivo* recordings from the same cell type: constraints can be added progressively, starting with *in vitro* recordings from dissociated neurons without dendrites, and proceeding to recordings from a slice preparation in which the dendrites are present but there is minimal synaptic activity, and finally to *in vivo* recordings from neurons that reflect the full complexity of a dynamic, non-stationary environment (Destexhe et al. 1996).

A number of attempts to systematize the process of parameter tuning have been described (e.g., Foster, Ungar, and Schwaber 1993; Bhalla and Bower 1993; Eichler-West and Wilcox 1995; Baldi, Vanier, and Bower 1996). The number of combinations of parameters that must be searched goes up exponentially with the number of parameters, so that in even the simplest one-compartment model with a few dozen parameters, an exhaustive search over all possible combination is simply not feasible. While there are ways to find optimal combinations of parameters in high-dimensional spaces, they suffer from both local minimum and uniqueness problems. A set of parameters may be locally optimal in the sense that making small changes to the parameters increases the error of the fit (Bhalla and Bower 1993), but there may be a better overall set of parameters in a different part of the parameter space that has not been tested. An approach based on genetic algorithms offers a way to make large jumps in the values of some combinations of parameters (Eichler-West and Wilcox 1995). The problem with uniqueness is that there may be many combinations of parameter values that fit the limited data equally well. Without a sufficiently rich set of data to constrain all the parameters in the model, it is impossible to have any confidence in the interpretation of the model.

The primary difficulty of systematic approaches based on optimization has been the time required to compute a single "evaluation function" (i.e., a simulation run)—typically seconds. Increases in computer performance are making these approaches more practical. In particular, the fastest supercomputers are multiple instruction, multiple data (MIMD) machines that have thousands of microprocessors. Because each processor can run the same simulation program with a different set of parame-

ters, taking full advantage of the computational power in a data-parallel way, these machines are ideal for exploring parameter spaces (see chapter 12, this volume).

A few general points are worth mentioning about confronting a complex model with thousands of parameters. First, there is a wide choice for the evaluation function, ranging from timing the occurrences of action potentials in response to current injection to matching statistical measures such as current-frequency curves (Foster, Ungar, and Schwaber 1993). Second, experimental data from a variety of conditions are needed to constrain most models, e.g., including the responses of neocortical neurons to fluctuating current injection, which is closer to *in vivo* conditions, as well as more conventional step current pulses (Mainen and Sejnowski 1995; Tang, Bartels, and Sejnowski 1997). Third, the problem of searching the space can be reduced to some extent by identifying parameters that covary; that is, the result may depend only on the ratios of some parameters, or on some other functional combination. A Bayesian framework offers a systematic way to take such dependencies into account (Baldi, Vanier, and Bower 1996). The most highly sensitive parameters in reproducing a particular result may be the most critical ones to constrain experimentally, and this may be one of the most important insights gained from the model.

Finally, if the goal of a model is to make a new discovery, in addition to summarizing existing data, the search for anomalies and failures of the model to fit aspects of the data may be more important than finding a perfect fit. When a model fails, the assumptions that went into constructing the model must be critically assessed, which can lead to new insights.

5.3 Applications

This section presents a few selected applications of compartmental models that have explored active dendritic function. Several examples have been chosen to illustrate how a detailed model helped to guide or illuminate electrophysiological studies along three lines of investigation: (1) synaptic integration in dendrites; (2) spike initiation and dendritic propagation; and (3) generation of firing patterns.

5.3.1 Synaptic Integration

Historically, dendrites have been seen as impeding current flow from synapses to the soma (Rinzel and Rall 1974). As a number of modeling studies have shown, synaptic inputs to distal dendritic locations suffer considerable attenuation in passive dendritic arbors of reconstructed neurons (Spruston et al. 1993; Zador, Agmon-Snir, and Segev 1995; Major et al. 1994; Mainen et al. 1996). A major role for excitable dendritic currents has been seen in boosting distal synaptic input to enhance its

propagation to the soma (Perkel and Perkel 1985; Shepherd et al. 1985; Pongracz 1985; Segev and Rall 1988; Jaslove 1992; Wathey et al. 1992).

The problem of synaptic attenuation and the possible role of active currents was addressed by Connors and colleagues (Cauler and Connors 1992; Amitai et al. 1993; Cauler and Connors 1994). Although it was found electrophysiologically that stimulation of layer-1 input to the distal tuft of layer-5 pyramidal cells could produce a surprisingly strong somatic excitatory postsynaptic potential (EPSP), a model neuron with a passive dendritic tree and massive layer-1 input could not reproduce a somatic EPSP as large as those observed experimentally (figure 5.2). Two problems contributed to weakening the effects of distal input on the soma:

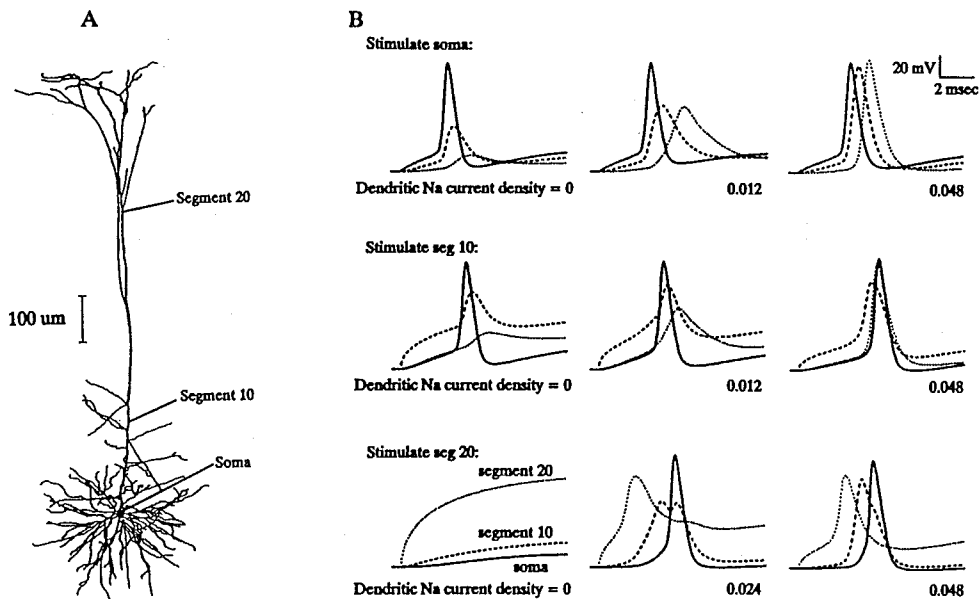


Figure 5.2 Simulations of soma-dendritic Na^+ spiking in a layer-5 pyramidal cell. (A) Camera lucida drawing of the modeled cell. Labels designate the locations of the three sites from which voltage changes are illustrated in panel B. (B) Effects of dendritic Na^+ channels and stimulus site on dendritic spiking; superimposed voltage responses from the soma (solid line), the trunk of the apical dendrite (segment 10; dashed line), and the end of apical trunk (segment 20; dotted line) while simulating with a step depolarizing pulse of current (intensity adjusted in each case to 1.5 times somatic spike threshold). Current was applied either at the soma (top row), to segment 10 (middle row), or to segment 20 (bottom row). Active Na^+ currents in the apical dendrites were assumed to be either absent (left column), at a relatively low density (middle column), or at a higher density (right column). Note that when the apical dendrites were passive (bottom left), it was not possible to bring the soma to spike threshold by stimulating segment 20, even when the local dendritic potential was positive.

1. The relatively high impedance of the distal branches leads to saturation of the synaptic current as the local membrane potential quickly depolarizes the neuron to near the synaptic reversal potential.
2. The cable properties (particularly the large axial resistance) of the dendritic arbor produce a large voltage drop between the distal site and the soma.

This anomaly between the model and the experimental results led to the hypothesis that low densities of Na^+ channels in the apical dendrite could boost layer-1 input enough to fire the cell (Cauler and Connors 1992; Amitai et al. 1993; Cauler and Connors 1994). This circumvents problem 2 by counteracting the voltage drop along the apical dendrite. Bernander, Koch, and Douglas (1994) expanded on this idea by tackling problem 1 in addition to problem 2. By adding a depolarization-activated outward current to the apical dendrite, their model compensated for saturation of synaptic current, helping to counteract the local depolarization produced by large inputs. They derived the voltage-dependence of a K^+ current necessary to accomplish exact linearization and showed that a biophysically reasonable K^+ current would be roughly suitable. Thus, in principle, a combination of Na^+ boosting and K^+ linearization could serve to compensate for the effects of the passive cable properties on synaptic input.

Recently, several physiological studies have directly tested the actual contribution of Na^+ currents to synaptic potentials (Stuart and Sakmann 1995; Schwindt and Crill 1995; Lipowsky, Gillessen, and Alzheimer 1996). Studying CA1 neurons, Lipowsky, Gillessen, and Alzheimer (1996) demonstrated that the amplitude of distal synaptic EPSPs, measured at the soma, was reduced by tetrodotoxin (TTX) locally applied to the apical dendrite (and to a much lesser extent by TTX applied to the axon or soma). Interestingly, the shape of the EPSP was not affected by TTX. To ensure that TTX was not acting presynaptically (TTX blocks presynaptic action potentials as well as postsynaptic Na^+ channels), they used a local field potential recording of the synaptic current (which was not affected by TTX) and postsynaptic hyperpolarization (which reduced the observed boosting). Examined in a compartmental model, these observations were consistent with physiological densities of I_{Na} in the main apical dendrite. Moreover, a dendritically located low-voltage-activated K^+ current was also needed to reproduce the data: specifically, to account for the lack of significant shape change of the boosted EPSPs.

In a study of layer-5 pyramidal cells, Stuart and Spruston (1995) also demonstrated the ability of a persistent Na^+ current to boost subthreshold synaptic currents, although they arrived at somewhat different conclusions about the location of the Na^+ channels contributing to the synaptic boost. Their technique was to use a

dendritic patch clamp electrode to inject current into the dendrite to mimic a synaptic current. This allowed them to use TTX to block I_{Na_p} . Interestingly, using local TTX application, they found that axosomatic Na^+ channels had a much greater effect than dendritic Na^+ channels in boosting the subthreshold current injection. Furthermore, dual axonic and somatic recordings showed that the site of greatest amplification was in fact the axon rather than the soma, consistent with suggestions that the axon initial segment contains a high density of Na^+ channels (Mainen et al. 1995; see also section 5.3.2). Schwindt and Crill (1995) also showed a contribution of I_{Na_p} to subthreshold amplification in layer-5 cells by examining the effect of TTX on iontophoretically applied pulses of glutamate.

One interpretation of the differences between these studies is a significantly different distribution of Na^+ channels between cortical layer-5 pyramidal cell and hippocampal CA1 pyramidal cells (Lipowsky, Gillessen, and Alzheimer 1996). The neocortical pyramidal cells may have a relatively higher axonal density of Na^+ channels.

Given the complexity and variety of the voltage-dependent Na^+ , Ca^{2+} , and K^+ channels in dendrites, the possibility arises that nonlinear synaptic integration more complex than amplification could occur. Even in the passive case, synaptic conductance changes could themselves cause current shunting and nonlinear interactions between nearby synapses (Rall 1964; Wang and Zhang 1996). Relative timing of a few milliseconds between neighboring excitatory and inhibitory synapses could significantly affect the current that reaches the spike-initiating region. (For a detailed model of the effects of voltage-dependent dendritic currents on synaptic integration in cerebellar Purkinje cells, see chapter 6, this volume.)

Before the properties of active dendritic conductances were firmly established, the theoretical possibility of performing logical operations (AND, OR, XOR) between synaptic inputs was explored with simulations (Shepherd and Brayton 1987; Rall and Segev 1987; Zador, Claiborne, and Brown 1992; Fromherz and Gaede 1993). A strictly logical function would be difficult to arrange, however, and low-order polynomial functions offer a more likely mathematical approximation to synaptic integration (Mel 1993). Sums of polynomial functions computed in different dendritic branches could be used to approximate a wide range of nonlinear functions, including the properties of complex cells in visual cortex (Mel, Ruderman, and Niebur 1996), which could be learned through long-term potentiation at excitatory synapses through activation of NMDA receptors (Mel 1992). This literature is necessarily more speculative and, thus far, less tied to physiological data (see Mel 1994 for a review). As recordings from dendrites become better refined, it should be possible to arrive at much better approximations to the types of spatial and temporal non-

linearities that neocortical neurons could compute. The results of these experiments may have profound implications for theories of function of the neocortex.

5.3.2 Spike Initiation

The initiation of an all-or-none action potential is the point at which a neural signal is transformed from analog to pulse-coded information. The site at which this transformation occurs is critical to the nature of signal processing carried out by a neuron. A number of modeling studies have examined the possibility of dendritic spike initiation (e.g., Shepherd et al. 1985; Softky and Koch 1993; Softky 1994). This work has been based less on physiological data than on the appeal of the richer computational properties offered by nonlinear processing in dendrites. For example, using simulations, Shepherd et al. (1985) showed that the presence of Hodgkin-Huxley conductances in dendritic spines could give rise to nonlinear interactions between neighboring synaptic inputs, as well as saltatory dendritic conduction of action potentials. Similarly, Softky (1994) modeled a mechanism for submillisecond synaptic coincidence detection based on brief dendritic spikes carried by fast Na^+ and K^+ currents. The relevance of speculative proposals such as these depends critically on resolving the actual locus of spike initiation.

In the classical description of spike initiation derived from the motoneuron, initiation normally occurs in proximal segments of the axon (in the region of the axon hillock or initial segment); when orthodromic stimulation is increased, the site of initiation may move into the dendrites (Coombs, Curtis, and Eccles 1957b; Fatt 1957; Fuortes, Frank, and Becker 1957). In the hippocampus and neocortex, the possibly greater excitability of pyramidal cell dendrites could tend to favor dendritic spike initiation (Spencer and Kandel 1961).

Both orthodromic and antidromic dendritic spike propagation in the hippocampus were described originally using current source density measurements (Richardson, Turner, and Miller 1987; Turner et al. 1991; Turner, Meyers, and Barker 1993). Dual dendritic/somatic recordings confirmed that the axon is a preferential site for spike initiation in neocortical and hippocampal pyramidal cells (Stuart and Sakmann 1994; Spruston, Jonas, and Sakmann 1995; Colbert and Johnston 1996), but that dendritic spike initiation can occur in mature animals during strong synaptic stimulation (Turner et al. 1991; Regehr et al. 1993; Stuart and Sakmann 1996).

When spikes initiate first in the axon, the action potential backpropagates into the dendritic tree (Turner et al. 1991; Stuart and Sakmann 1994). This antidromically propagating action potential could signal the firing time of the neuron throughout the dendritic arbor, leading, for example, to Hebbian plasticity (Markram et al. 1997; Magee and Johnston 1997). The degree of invasion of the backpropagating

action potential is not fixed (Spruston, Jonas, and Sakmann 1995; Svoboda et al. 1997) but can be regulated through Na^+ channel inactivation by previous spikes (modeled by Migliore 1996), K^+ channel activation, excitatory (Magee and Johnston 1997; Hoffman et al. 1997) or inhibitory (Buzsaki et al. 1996; Tsubokawa and Ross 1996) synaptic potentials, and, potentially, neuromodulators such as acetylcholine, norepinephrine, and serotonin.

Two recent modeling studies of spike initiation have attempted to account for the above experimental results using known anatomical and physiological properties of pyramidal cells (Mainen et al. 1995; Rapp, Yarom, and Segev 1996). Both studies used reconstructed cortical neurons and just two voltage-dependent currents, I_{Na} and I_{Kd} , assuming that the contributions from the other currents would not be significant during on the short time scale of spike initiation. The conclusions of the two studies were similar (figure 5.3):

1. The passive electrical load biases the neuron toward spike propagation in the antidromic direction. This is analogous to the greater ease with which a voltage signal is passed outward from the soma than inward toward the soma, (see chapter 2, this volume) although geometrical considerations alone are insufficient to account for a strong bias for axonal initiation.
2. The presence of a larger source of Na^+ current—either a very high density (Mainen et al. 1995) or a moderate density with altered kinetics (Rapp, Yarom, and Segev 1996)—in the axon initial segment can account for preferential axonal initiation (but compare with Colbert and Johnston 1996, discussed earlier).
3. Although density measurements for the dendritic and somatic Na^+ channels are similar (Stuart and Sakmann 1994), the experimentally observed decrement of the backpropagating spike can be reproduced because this density is low. The axonal Na^+ source serves to increase the amplitude of the somatic action potential.
4. A developmental increase in Na^+ density (Huguenard, Hamill, and Prince 1988) can account for the increased tendency toward dendritic initiation in older animals (Stuart and Sakmann 1996).

A recent physiological study (Hoffman et al. 1997) has shown that dendritic K^+ channels may also have a major role in the locus of initiation and control of dendritic action potential. An enrichment of an I_A -like current in the dendritic arbor (Maletic-Savatic, Lenn, and Trimmer 1995) can limit the size of transient events such as EPSPs and spikes, thereby shunting dendritic spikes. By activating during the rising phase of the action potential, this current could also reduce the amplitude of a backpropagating spike, allowing for a relatively higher dendritic Na^+ current

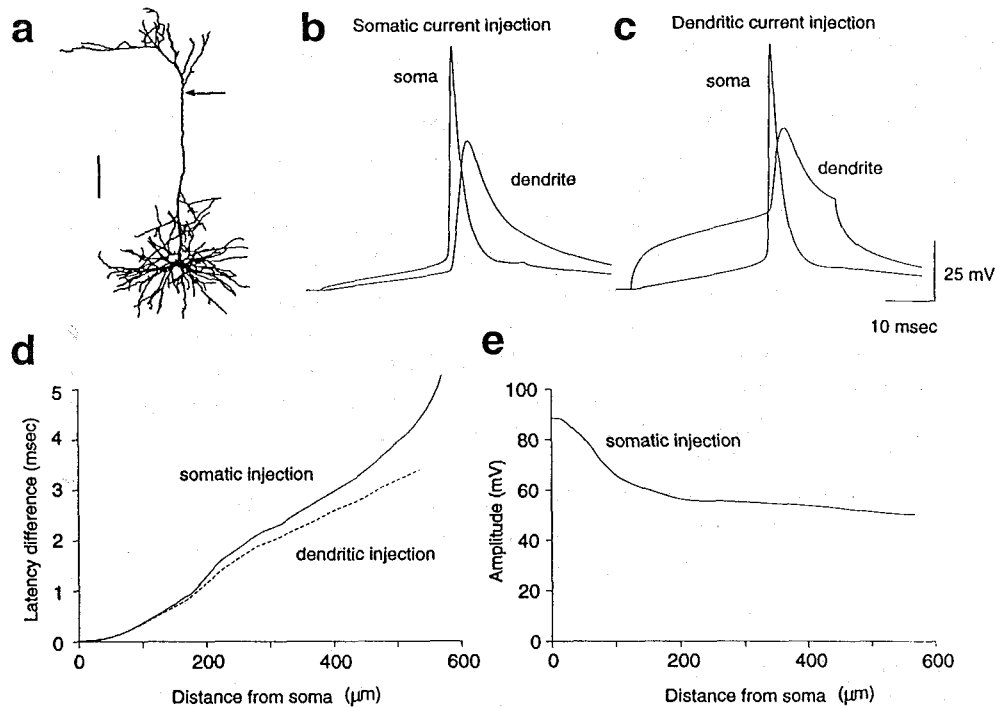


Figure 5.3

Site of action potential initiation in a model of a neocortical pyramidal neuron (compare to Stuart and Sakmann 1994, figure 1). (a) Digitally reconstructed layer-5 pyramidal neuron (courtesy of D. K. Smetters and S. Nelson, unpublished). Arrow indicates dendritic recording/stimulation site in panels b–c. Scale bar is 100 μm . (b) Simulation of action potentials evoked by a current step injected at the soma. Voltage traces from the soma and apical dendrite are shown. (c) Similar to panel b, but current injection is made at the dendritic site. (d) Latency difference between peak somatic and peak dendritic potential at different distances from the soma. Action potentials were elicited by somatic (solid line) or dendritic (dashed line) current injection. Latencies were measured using time-to-peak amplitude. (e) Action potential amplitude plotted as function of distance from the soma under the same conditions as in panel b following somatic injection. This figure is based on Mainen et al. 1995. NEURON code, including “.mod” files describing the active currents and “.hoc” code describing the morphologies and simulation setup, used to generate this figure is available; see “Internet Resources.”

density, even while maintaining a decremental antidromic invasion (Hoffman et al. 1997).

In contrast to the many models that explore the consequences of Na^+ and Ca^{2+} currents in dendrites, models that explore the functional roles of dendritic K^+ currents have been few (e.g., Wilson 1995; Hoffman et al. 1997), in part because patch recordings and anatomical studies of K^+ currents are not as far advanced (Softky and Koch 1993; Bernander, Koch, and Douglas 1994; Wilson 1995; Andreassen and Lambert 1995). Both Rapp, Yarom, and Segev (1996) and Mainen et al. (1995) used a low density of dendritic K^+ channels to reproduce the relatively slow repolarization of the dendritic spike and the lack of AHP in the dendrites (Stuart and Sakmann 1994). However an I_A that inactivates rapidly enough may exert its influence primarily on the upstroke of a dendritic spike and become inactivated without contributing to a fast repolarization or AHP (Hoffman et al. 1997).

Given the importance of spike initiation for cortical signaling—all the information that flows into, out of, and between cortical areas is coded by spike trains—the axon hillock and initial segment deserve much more attention.

5.3.3 Intrinsic Firing Patterns

Different types of neurons produce different intrinsic rhythmic firing patterns when stimulated with a simple depolarizing current pulse *in vitro* in the absence of synaptic activity. For pyramidal neurons, these intrinsic patterns are typically either bursting (stereotyped clusters of two or more spikes firing at rates of up to 1,000 Hz) or adapting (firing at rapidly or gradually slowing rates; McCormick et al. 1985). The impression of these intrinsic properties can be seen in the characteristic firing modes of different types of neurons *in vivo* (e.g., complex spikes fired by hippocampal pyramidal cells, which reflect their intrinsic bursting properties). Thus the temporal pattern of spikes emitted by a neuron *in vivo* reflects both the pattern of synaptic and modulatory input the neuron receives and the sculpting of this input by the dendritic, somatic, and axonal conductances that generate the spike train (Llinás 1988).

Modeling (and experimental) studies have begun to explore three important issues in the relationship between intrinsic firing patterns and neural signaling:

1. How are intrinsic firing patterns determined by the interplay of intrinsic conductances and neural geometry (see below)?
2. How do intrinsic currents interact with synaptic currents (e.g., Reyes and Fetz 1993; De Schutter and Bower 1994b, 1994c; Jaeger, De Schutter, and Bower 1997; Mainen and Sejnowski 1995; Tang, Bartels, and Sejnowski 1997)?

3. How do different temporal spike patterns interact with the filtering characteristics of synaptic transmission (e.g., Markram and Tsodyks 1996; Tsodyks and Markram 1997; Abbott et al. 1997; Lisman 1997)?

While all three issues are crucial to understanding the propagation of a neural signal, with respect to the modeling literature, the first is by far the best developed.

Models of bursting and repetitive firing in pyramidal neurons were pioneered by Traub and colleagues (Traub and Llinás 1979; Traub 1979, 1982; Traub et al. 1991, 1994). The original Traub model (Traub and Llinás 1979) laid out basic mechanisms by which slow dendritic Ca^{2+} and K^+ channels, partially coupled with somatic Na^+ channels, gave rise to rhythmic bursting in hippocampal pyramidal neurons. This model also documented the ability of dendritic Na^+ "hot spots" on fine dendrites to produce the fast prepotentials described in these neurons (Spencer and Kandel 1961). A revision of this model (Traub 1982) was constructed to account for data showing bursts generated locally in the dendrites (Wong, Prince, and Basbaum 1979); this required the addition of dendritic inactivating K^+ conductances (I_A), a prediction that appears to have been borne out by the recent data (Hoffman et al. 1997).

The elaboration of the bursting model in Traub et al. (1994), which included an axon and more complex dendrites, combined synaptic and intrinsic voltage-dependent conductances. Versions of the Traub model have served as the starting point for other models aimed at exploring the influence of intrinsic properties of neurons on the interactions between neurons in area CA3 of the hippocampus. The model CA3 pyramidal neuron was also modified to serve as a CA1 pyramidal neuron by increasing I_{Kd} and decreasing dendritic I_{Ca} and I_C . After these alterations, tonic depolarization of the soma leads to adapting repetitive firing, whereas stimulation of the distal dendrites leads to bursting. A related model of bursting in neocortical neurons emphasized the importance of dendritic I_{Na} in propagating the somatic spike into the dendrites to trigger I_{Ca} (Rhodes and Gray 1994). Bursting in this model depended critically on the amount of I_{AHP} activation, and hence on the level of intracellular Ca^{2+} .

In these models of bursting, the Ca^{2+} currents in the dendrites produce the prolonged depolarization that initiates the fast Na^+ spikes, but there is increasing evidence that Na^+ currents themselves can produce bursts in some neurons (Turner et al. 1994; Franceschetti et al. 1995; Azouz, Jensen, and Yaari 1996). Because Na^+ currents are quite brief, the longer time scale of the burst must arise somehow from the geometry of the neuron and the interaction between different conductances in different compartments. Using reconstructed cortical neurons with different dendritic structures but a fixed distribution of ion channels, Mainen and Sejnowski (1996)

have shown that the entire range of intrinsic firing patterns, including nonadapting, adapting, and bursting types, can be reproduced in a set of neurons that differ only in their geometry (figure 5.4). In their study, reconstructed layer-5 pyramidal cells with large dendritic arbors produced repetitive bursting to current injection, while more compact layer 2/3 pyramidal cells produced regular spiking behavior. These results demonstrated that the electrotonic structure of a neuron shapes the dynamic interactions between nonuniformly distributed ion channels, and may thereby shape the pattern of repetitive firing. The wide anatomical variety of neocortical dendrites (Peters and Jones 1984), supported the idea of a continuous spectrum of neocortical firing patterns (McCormick et al. 1985; Connors and Gutnick 1990), rather than discrete categories.

Mainen and Sejnowski (1996) suggested a causal relationship for the observed correlations between dendritic structure and firing properties (Connors and Gutnick 1990; Chagnac-Amitai, Luhmann, and Prince 1990; Mason and Larkman 1990; Franceschetti et al. 1995; Yang, Seamans, and Gorelova 1996) and emphasized the importance of active dendritic conductances in neuronal function. Quadroni and Knöpfel (1994) have also demonstrated in simulations that the number of dendrites may affect the firing patterns of medial vestibular neurons. Heterogeneity of dendritic structure can thus parsimoniously explain some aspects of the heterogeneous firing properties of neurons in terms of their anatomical diversity, but heterogeneity in the distribution of channel may also be important. Indeed, a modeling study by Migliore, Alicata, and Ayala (1995) demonstrated that the effects of small differences in morphology can be overridden by tuning the relative densities of intrinsic currents such as sI_{AHP} .

Most of these models are based on data from cortical slices that lack the spontaneous background firing activity and tonic neuromodulation that occurs in vivo. Models that take these conditions into account (Bernander et al. 1991; Rapp, Yarom, and Segev 1992; Tang, Bartels, and Sejnowski 1997) may reveal other properties of neurons that are important for their participation in perceptual and cognitive states.

5.4 Analysis

This chapter has focused on highly detailed models of pyramidal cells derived from anatomical and physiological data. The resulting models of active dendritic processes are complex, yet, however exhaustively their behavior may be scrutinized, new tools for analysis may be needed to achieve a deeper understanding of the phenomena they display. The development of these methods is still nascent, but several useful avenues are worth mentioning.

5.4.1 Reduced Models

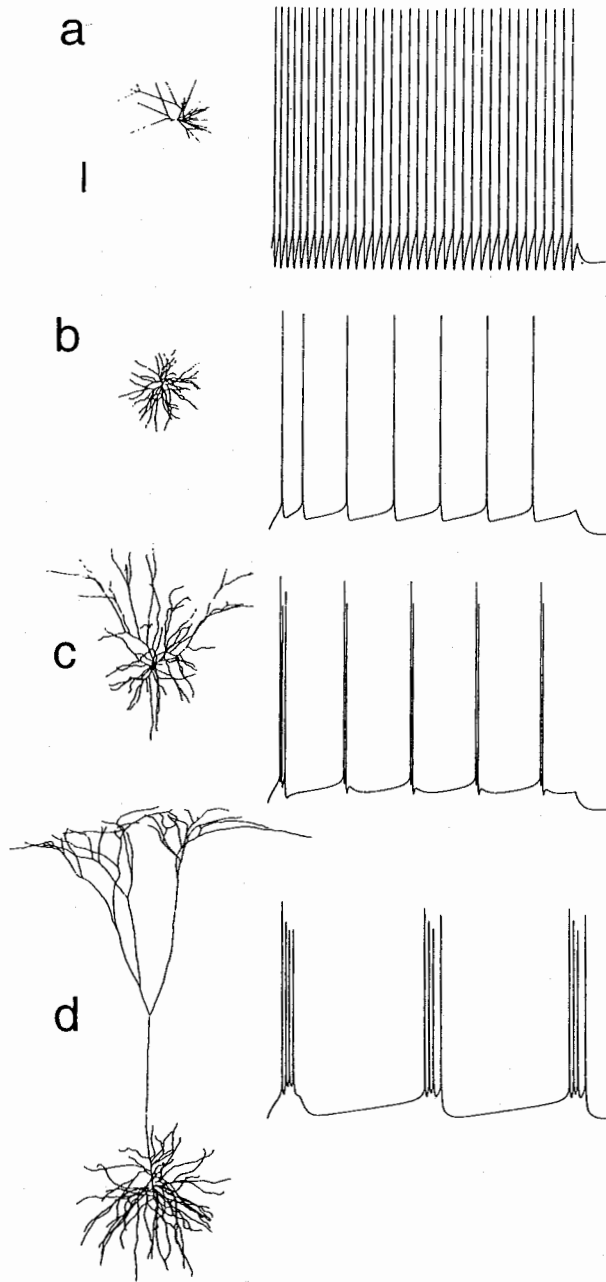
If the complex behavior of a realistic model can be captured in a much simplified version of the model, understanding of the model can be enormously improved. Collapsing the number of compartments in a model is a good starting point for simplification. For passive electrical structures, several straightforward methods are discussed in chapter 3, this volume. With active models, reducing both the number of active conductances and the number of compartments may be useful (e.g., Lytton and Sejnowski 1991; chapter 10, this volume).

A single-compartment model will be sufficient when the electrotonic structure of the neuron is not relevant to its behavior, but otherwise, a minimal model consists of two compartments. Pinsky and Rinzel (1994) developed a simplification of the model of Traub et al. (1991) with just two compartments, identified as a soma and a dendrite. The electrical geometry was reduced to two parameters: the ratio of soma to dendrite area, ρ ; and the coupling resistance between them, κ . Despite this simplicity, the model captured essential aspects of the generation of bursting in the Traub model not found in a single-compartment model (Pinsky and Rinzel 1994). The reduced number of parameters allows the model to be used efficiently in network simulations and aids in understanding the role played by electrical structure in the behavior of the model. (See more in chapter 10, this volume.)

Mainen and Sejnowski (1996) also used a two-compartment model similar to that of Pinsky and Rinzel (1994) to elucidate the effects of electrical geometry on the firing patterns of neocortical neurons. The full range of regular spiking responses, adaptation, afterdepolarizations, and repetitive bursting observed in recordings and in models of reconstructed pyramidal cells and inhibitory neurons could be reproduced in the two-compartment model. This reduced model shed light on the mechanisms responsible for the effects of geometry on the spike firing pattern observed in more detailed models of reconstructed neurons.

5.4.2 Current-Voltage Curves

One of the more informative analyses for understanding how a model neuron will respond to inputs is the current-voltage relationship (I - V curve). Because data from experimental recordings are often presented in this way, the I - V curve of the model can be compared directly with measurements. The steady-state, or static I - V curve, $I_{\infty}^{static}(V_m)$, is obtained by voltage clamping the soma to V_m and determining the asymptotic current. The slope of this curve defines the steady-state input conductance of the neuron as a function of membrane potential. The momentary, or instantaneous, I - V curve, $I_O(V_m)$, is obtained by changing the membrane potential



rapidly from the resting level to a new value, V_m , more rapidly than all the conductances (except for I_{Na} , which has an activation time of less than 100 μsec).

Koch, Bernander, and Douglas (1995) have analyzed the threshold of a model cortical pyramidal cell using the I - V relationships (figure 5.5). Near the spiking threshold, there is a local maximum in the $I_{\infty}^{\text{static}}(V_m)$, which corresponds to the current threshold for sustained inputs. The voltage threshold, which applies to rapid synaptic currents or current injection, occurs at a zero-crossing of $I_O(V_m)$, which is more depolarized than $I_{\infty}^{\text{static}}(V_m)$. Koch, Bernander, and Douglas (1995) define a third, dynamic I - V relationship, while the cell is spiking. The relationship between current inputs in the dendrites and spiking in the soma can also be studied using similar techniques (Jaeger, De Schutter, and Bower 1997).

5.4.3 Phase Plane Analysis

Because the previous histories of the ionic currents are also important in determining the response of a neuron to an input, the I - V curves defined above only give a rough idea of how a cell will respond to a more complex time-varying input. Hysteresis occurs already at the start of a simulation because the states of the activation and inactivation variables of all the ionic currents affect the subsequent dynamics. Phase plane analysis can be used to visualize and analyze the complex dynamics exhibited by neurons during simulations.

The “phase” in phase plane analysis refers to variables such as the membrane potential and current that dynamically change during a simulation but it also includes other variables such as the activation and inactivation variables for the ionic currents and ion concentrations. In the phase plane of current against membrane potential, the neuron follows a trajectory on a two-dimensional graph (see chapter 7, this volume). The current through specific channels or the internal Ca^{2+} concentration can also serve as axes in a phase plane. For example, Lytton and Sejnowski

Figure 5.4

Distinct firing patterns in model neurons with identical channel distributions but different dendritic morphology. Digital reconstructions of dendritic arbors of neurons from rat somatosensory cortex (panel a) and cat visual cortex (panels b–d). (a) Layer-3 aspiny stellate. (b) Layer-4 spiny stellate. (c) Layer-3 pyramid. (d) Layer-5 pyramid. Somatic current injection evoked characteristic firing patterns. Panel a shows only the branch lengths and connectivity, while panels b–d show a two-dimensional projection of the three-dimensional reconstruction. Scale bars: 250 μm (anatomy), 100 msec, 25 mV. Dendritic reconstructions were provided by J. Anderson, K. Martin, R. Douglas, L. Cauler, and B. Connors. Active conductances included four active currents: I_{Na} from Mainen et al. 1995; I_{Kd} from Mainen et al. 1995; I_M from Gutfreund, Yarom, and Segev 1995; I_{Ca} from Reuveni et al. 1993; and sI_{AHP} from Reuveni et al. 1993. This figure is based on Mainen and Sejnowski 1996. NEURON code, including “.mod” files describing the active currents and “.hoc” code describing the morphologies and simulation setup, used to generate this figure is available; see “Internet Resources.”

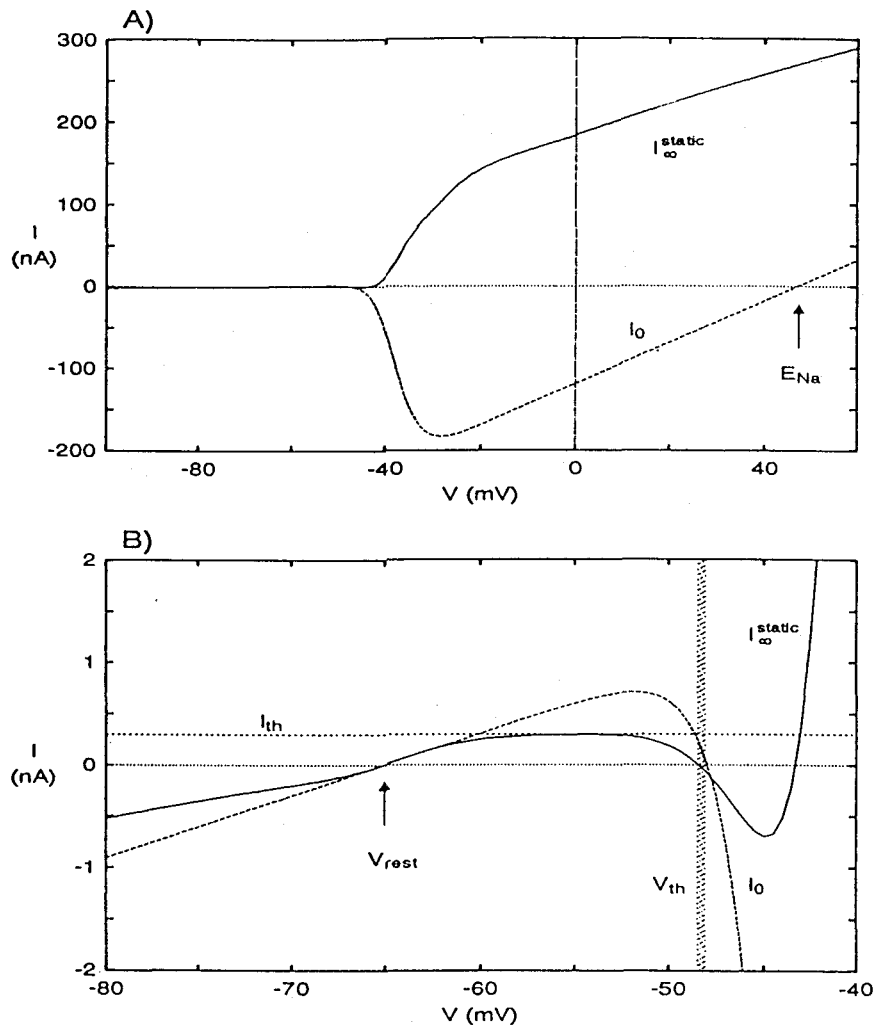


Figure 5.5

Current-voltage relationship for a model cell (Koch, Bernabe and Douglas, 1995). The somatic membrane potential V_m was voltage-clamped and the clamp current ' $I_{\infty}^{static}(V_m)$ ', recorded once steady state was reached. The instantaneous current-voltage curve ' $I_0(V_m)$ ', assumes that the membrane potential is instantaneously displaced from V_{rest} to its new value at V_m . All somatic membrane conductances retain the values they had at V_{rest} with the sole exception of the fast sodium activation process—due to its very fast time constant (50 μ sec) we assume that it reaches its steady-state value at V_m . (A) Full range. Note the very large amplitudes of I_0 (due to I_{Na} activation) and of $I_{\infty}^{static}(V_m)$ (due to I_{Dr} activation). The instantaneous current I_0 crosses over close to the reversal potential for I_{Na} . (B) Detail of panel A in the vicinity of the resting potential and spike threshold. Both curves reverse at V_{rest} . The slope of $I_{\infty}^{static}(V_m)$ corresponds to the inverse of the input resistance at rest. The right zero-crossing of I_0 occurs at $V_m = -48$ mV and that of $I_{\infty}^{static}(V_m)$ at -48.5 mV. The amplitude of $I_{\infty}^{static}(V_m)$ at the local peak around -54 mV represents the current threshold, I_{th} , for spike initiation, while the location of the middle zero-crossing of I_0 corresponds to the voltage threshold V_{th} for spike initiation (indicated by the thin gray area).

(1991) used phase plane analysis with these variables to explore the entrainment of cortical pyramidal neurons by inhibitory postsynaptic potentials. In some cases it is possible to gain a qualitative feel for the dynamics by plotting the null clines on the phase plane, which correspond to lines along which the derivatives of variables are zero (Murray 1989).

Phase plane analysis can reveal more about the mechanisms underlying dynamics through the application of bifurcation theory. As one parameter, such as input current or a conductance, is changed slowly, the phase plane trajectory for a repetitively firing neuron may qualitatively shift, for example, from a regular spiking mode to a bursting mode (see chapter 7, this volume; Butera, Clark, and Byrne 1996). This sudden shift indicates that a bifurcation has occurred in the dynamics; that is, a discontinuous change in the behavior of the system. In the theory of dynamical systems, the types of bifurcations that can occur have been classified and analyzed. Although this approach is normally used on simplified models of neurons that can be characterized by a few differential equations, new automated software systems such as XPP (Bard Ermentrout; see chapter 7, this volume; <ftp://ftp.math.pitt.edu/pub/bardware/tut/start.htm>) and "DsTool" (John Guckenheimer; <ftp://macomb.tn.cornell.edu/pub/dstool>) make it feasible to analyze the bifurcations in more realistic models systems represented by dozens of differential equations.

Internet Resources

An increasing number of valuable resources are available on the Internet. At our web site, <http://www.cnl.salk.edu/CNL/simulations/methods.html>, we have compiled a directory that includes code used to generate several of the models illustrated here (figures 5.3 and 5.4), as well as links to simulation software (e.g., NEURON and GENESIS) and models. This directory will be periodically updated.

Acknowledgments

The preparation of this chapter was supported by Howard Hughes Medical Institute, National Institutes of Health, and the Office of Naval Research. We are grateful to Venkatesh Murthy and Brian Christie for comments on this chapter.